

**1992 NASA/ASEE SUMMER FACULTY FELLOWSHIP PROGRAM**

**JOHN F. KENNEDY SPACE CENTER  
UNIVERSITY OF CENTRAL FLORIDA**

**USE OF CYCLIC CURRENT REVERSAL POLARIZATION VOLTAMMETRY FOR  
INVESTIGATING THE RELATIONSHIP BETWEEN CORROSION RESISTANCE AND  
HEAT-TREATMENT INDUCED VARIATIONS IN MICROSTRUCTURES OF  
440C MARTENSITIC STAINLESS STEELS**

<b>PREPARED BY:</b>	<b>Dr. John R. Ambrose</b>
<b>ACADEMIC RANK:</b>	<b>Associate Professor</b>
<b>UNIVERSITY AND DEPARTMENT:</b>	<b>University of Florida Department of Materials Science and Engineering</b>
<b>NASA/KSC</b>	
<b>DIVISION:</b>	<b>Materials Science Laboratory</b>
<b>BRANCH:</b>	<b>Failure Analysis and Materials Evaluation</b>
<b>NASA COLLEAGUE:</b>	<b>Coleman J. Bryan</b>
<b>DATE:</b>	<b>July 24, 1992</b>
<b>CONTRACT NUMBER:</b>	<b>University of Central Florida NASA-NGT-60002 Supplement: 8</b>

## ACKNOWLEDGEMENTS

I would like to express my appreciation for again being selected to participate in the 1992 NASA/ASEE Summer Faculty Fellowship program, to Loren Anderson [University of Central Florida] and Carol Valdes [NASA] for their capable administration of the program, and to my NASA colleagues Cole Bryan and Rupert Lee for their assistance and encouragement. In many ways, this second year was more fulfilling than the first - it was surely more challenging. I thank Lewis MacDowell for the opportunity to use his equipment and see how our tax money goes to buy the kind of equipment the State of Florida chooses not to supply its universities with - also for his help in that critical stage of data transfer. To Steve McDanel, my thanks for your SEM work; to Scott Murray, our all too few trips outside the O & C building were always welcome. And to Peter Marciniak and the rest of the endangered wildlife on Merritt Island...thanks for letting me be a part of your day.

## ABSTRACT

Software for running a cyclic current reversal polarization voltammogram has been developed for use with a EG&G Princeton Applied Research Model 273 potentiostat/galvanostat system. The program, which controls the magnitude, direction and duration of an impressed galvanostatic current, will produce data in ASCII format which can be directly incorporated into commercial spreadsheets [Lotus, Quattro] for graphical representation of CCRPV voltammograms.

The program was used to determine differences in corrosion resistance of 440C martensitic stainless steel produced as a result of changes in microstructure effected by tempering. It was determined that tempering at all temperatures above 400°F resulted in increased polarizability of the material, with the increased likelihood that pitting would be initiated upon exposure to marine environments.

These results will be used in development of remedial procedures for lowering the susceptibility of these alloys toward the stress corrosion cracking experienced in bearings used in high pressure oxygen turbopumps used in the main engines of space shuttle orbiters.

## **SUMMARY**

1. Description and rationale of the cyclic current reversal polarization voltammetry technique are presented.
2. Development of a program with which a commercial potentiostat can be menu driven, using a PC to run the experiment, to acquire and to process the data.
3. The technique and experimentation procedure were tested against alloys whose microstructure had been changed by heat treatment. Results will be used to develop other, more effective, heat treatment procedures.

## TABLE of CONTENTS

- 1.0 INTRODUCTION
  - 1.1 EXPERIMENTAL BASIS FOR EXPERIMENTAL PROCEDURE
  - 1.2 CRITERIA FOR CORROSION SUSCEPTIBILITY
  - 1.3 PROPOSED EXPERIMENTAL PROTOCOL
- 2.0 EXPERIMENTAL - MATERIALS AND EQUIPMENT
  - 2.1 Materials
  - 2.2 Equipment
  - 2.3 Experimental Procedure
- 3.0 EXPERIMENTAL RESULTS AND DISCUSSION
- 4.0 CONCLUSIONS
- 5.0 RECOMMENDATIONS FOR FUTURE WORK
- 6.0 APPENDICES
  - 6.1 Appendix A
  - 6.2 Appendix B

## LIST OF ILLUSTRATIONS

<u>Figure</u>	<u>Title</u>
1	Schematic of a single cycle CCRPV sweep and associated interpretive parameters.
2	Schematic of multiple CCRPV cycles and interpretive output parameters.
3	Schematic representation of limiting cases in polarization behavior - metal dissolution v. insoluble corrosion product.
4	Schematic of Experimental Procedure with respect to the CCRPV control variables.
5	Plot of Degree of Polarization $[V(t)-V(o)]$ v. $t^{\frac{1}{2}}$ for all four 440C tempers - 1st anodic cycle, 1st CCRPV group.
6	400° temper, group 1 anodic cycles.
7	750° temper, group 1 anodic cycles.
8	1000° temper, group 1 anodic cycles.
9	1250° temper, group 1 anodic cycles.
10	Group 1, 1st cathodic cycles for 400°, 750°, 1000° and 1250° tempers.
11	400° temper, group 1 cathodic cycles.
12	750° temper, group 1 cathodic cycles.
13	1000° temper, group 1 cathodic cycles.
14	1250° temper, group 1 cathodic cycles.
15	Comparison of 5th anodic cycles in groups 1-3 for temper 400°.
16	Comparison of anodic cycles for groups 1-3 for temper 750°.
17	Temper 1250, comparison of 5th anodic cycles, groups 1-3.
18	1000° temper, comparison of 5th anodic cycles for groups 1-3.
19	400 temper, comparison of 5th cathodic cycles, groups 1-3.

- 20 750 temper, comparison of 5th cathodic cycles for groups 1-3.
- 21 1000° temper - comparison of 5th cathodic cycles for groups 1-3.
- 22 1250 temper - comparison of 5th cathodic cycles for groups 1-3.



## 1.0 INTRODUCTION

There have been a number of occurrences of stress corrosion cracking [SCC] failures of AISI 440C cryogenic bearing races, a component of Pratt and Whitney high pressure oxygen turbopumps [HPOTP] used in the main engines of the space shuttle orbiter main engines. Stress Corrosion Cracking is a localized corrosion phenomenon involving propagation of cracks through the cross-section of a material due to the interaction of an applied or residual stress upon exposure to certain environments. Failures appear to result from a synergistic interaction of three variables, namely:

1. Surface Finish [roughness] produced by grinding,
2. "Non-Optimal" microstructure produced by quenching and
3. Susceptibility of this alloy composition toward chloride induced environmental fracture.

A number of fabrication modifications which change these particular variables have been shown to result in extended service life or time to failure [TTF]. Since selection of an alternate material is out of the question at this point in time, attention has focussed on procedures which increase the time to failure for the material.

One possibility would be to increase SCC resistance by increasing the temperature used in tempering the martensitic microstructure produced during the quench from the austenitization temperature. The beneficial aspects of this procedure involve a minimization of "...residual quench tensile stresses while producing a less brittle martensite." [quotation from Pratt-Whitney audio-visual presentation AVA376070 901005]. However, the effect of this variation with respect to corrosion resistance has yet to be resolved. It should be emphasized that true SCC susceptibility is determined by electrochemical/mechanical testing methodology. However, the standard test methodology - slow strain rate testing - is a prohibitively long test. The question is - can an accelerated electrochemical test procedure which has successfully been used to differentiate between degrees of susceptibility to SCC possess sufficient sensitivity to determine the effectiveness of these remedial fabrication procedures?

## 1.1 THEORETICAL BASIS for PROPOSED EXPERIMENTAL PROCEDURE

Measurement of degree of polarization which result from impressed current is not a new technique, having been used for some time as an analytical chemistry technique - chronopotentiometry, stripping voltammetry, etc. It has not been

used to any great extent in corrosion science applications. It would seem, however, to be most appropriate in measuring the behavior of a material in response to flow of current across the metal/environment interface. By impressing a constant [galvanostatic] current between an inert electrode [platinum counter] and the material being characterized [working electrode], the potential change or polarization can be measured as a function both of time and of the amplitude of the impressed current. In order to simulate "natural" conditions, the current direction should be regularly reversed in order to develop concentrations of both kinds of reaction products at the metal interface - anodic and cathodic. Thus evolves the name of the technique - "CYCLIC CURRENT REVERSAL POLARIZATION VOLTAMMETRY" or CCRPV. The experimental variable to be measured will be the rate of change in material potential, or "polarization rate".

### Cyclic Current Reversal Polarization Voltammetry [CCRPV]

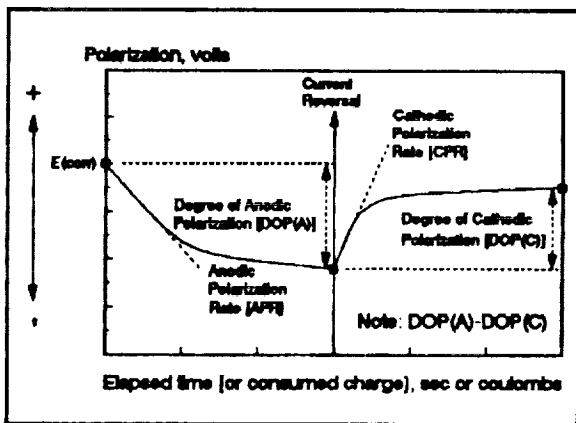


Figure PRATT-1 - Schematic of a single cycle CCRPV sweep and associated interpretive parameters.

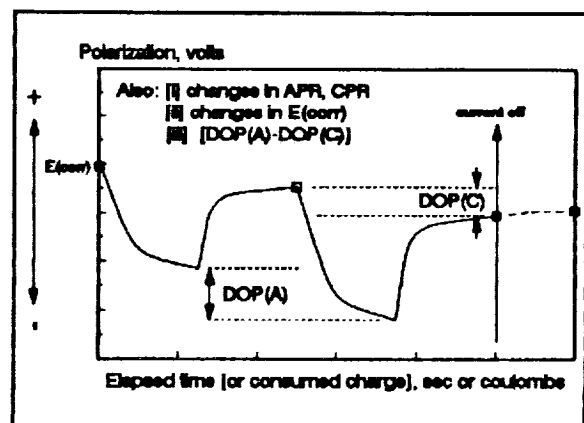


Figure PRATT-2 - Schematic of multiple CCRPV cycles and interpretive output parameters.

The experimental methodology for the CCRPV technique is quite simple, utilizing a conventional potentiostat in the galvanostatic mode coupled to a square wave signal generator and an oscilloscope for measuring polarization kinetics. This polarization rate output for both single and multiple cycles contains a variety of types of information which relates directly to the corrosion process [Figures PRATT-1 and PRATT-2]. The various output parameters which will be utilized in determination of electrolyte corrosivity are discussed below.

Degree of polarization [DOP] is given by the magnitude of potential shift [polarization] associated with a particular direction of impressed current flow - i.e. for an anodic impressed galvanostatic pulse, the degree of anodic polarization

[DOP(A)] is given by:

$DOP(A) = E_A - E_s$ , where  $E_A$  = the potential of the working electrode at the end of a given current pulse, and  
 $E_s$  = the potential at the start of the current pulse.

A large value for DOP(i) indicates the presence of a large resistive component in the current path between counter [auxiliary] and working electrodes. Although consistent with the occurrence of a protective surface barrier layer, a large electronic resistance does not, by itself, guarantee equivalent corrosion resistance. First, passivity is usually associated with ionic resistance of insoluble corrosion products. Secondly, large degrees of electronic resistance can often result in dielectric breakdown of passive layers with associated high localized corrosion rates - e.g. pitting above pitting potentials, etc.

Anodic and Cathodic Polarization Rates [APR and CPR], determined from polarization v. time plots, are directly related to changes in resistance toward charge transfer [metal dissolution (A) or plating (C)] rates and to kinetics of insoluble film growth (A) or dissolution (C). Normally, these processes may be distinguished using Rotating Ring-Disc voltammetry techniques. However, in the proposed experimentation, only progressive changes in polarization kinetics will be used as a quantitative measure for stability of the system. Any potential arrests occurring during the polarization transient can be related to the electrochemical reactions responsible for the consumption of current by associating the potential arrest with a variation in the kinetics of a particular Redox process.

$E_s$  potentials, particularly progressive shifts in rest potentials are directly related to variations in corrosion potential  $E_{corr}$ . Although variations in corrosion potential have often been considered as "irreproducible" behavior by the uninitiated, these shifts are, in fact, associated with an irreversible component of the total polarization which occurs in response to the passage of current. The direction and magnitude of these  $E_s$  potentials can be related to the process[es] responsible for their occurrence by comparing their behavior in response to changes in other experimental variables - i.e. solution flow rate, amplitude and frequency of current pulses, etc.

System stability [or, alternatively, system corrosivity] can be estimated by associating progressive changes in one or more of these parameters with changes in the subject material - with surface roughness or microstructure, for example. We have demonstrated that austenitic stainless steels found to be sensitive to pitting or to intergranular stress corrosion

cracking were easily polarized with but a few current reversal cycles to potentials above a critical value for initiation of pits. For these stainless steels, onset of pitting - and presumably SCC crack initiation as well - was signalled by an abrupt decrease in polarization once this critical value was exceeded. This procedure was also effective in correlating a decreased pitting resistance with the amount of retained delta ferrite in the weldments of 316L austenitic stainless steels.

We should be reminded that susceptibility to SCC is determined by mutually inclusive electrochemical and mechanical factors - breakdown of passivity is one factor. However, the mechanical factor cannot be ignored. What we are assuming here is that the material is intrinsically susceptible - 440C martensitic stainless steel will eventually fail by SCC. We are will be trying to determine whether remedial fabrication methodology [1] affects resistance to passivity breakdown and [2] whether such change in resistance can be detected by our proposed experimental protocol. The "bottom line" will be - can a "calibration curve" of sorts be constructed which demonstrates a some direct relationship between a processing variable [e.g. surface polishing, "pancake" forging or temperature induced microstructural alteration] and a measure of localized corrosion resistance.

## 1.2 CRITERIA for CORROSION SUSCEPTIBILITY EVALUATION

Polarization in response to current flow can be of three types, individually or in combination:

- i. a potential drop across an ohmic resistance. This polarization is characterized by a  $V=IR$  response, and is virtually time independent - i.e. instantaneous polarization with application of current. Capacitance or interfacial charging processes are included in this category as is the voltage drop across the electrolyte between the working and counter electrodes.
- ii. polarization due to the resistance to charge transfer across the electrified interface - i.e. so-called "Tafel" overvoltage. This kind of polarization is characterized by a logarithmic dependence upon current flow - the "Tafel Equation":

$$\ln [I] - \eta_1 \left[ \frac{\eta_1}{\beta_1} \right]$$

where  $n_i$  = degree of polarization produced by current  $I$   
 and  $\beta_i$  = charge transfer resistance.

- iii. the potential drop across an insoluble reaction product or film which forms at the metal/electrolyte interface. The degree of polarization is a function of the resistivity of the reaction product, the polarization rate is a function of the nucleation/growth kinetics of the deposition process. It is this polarization process with which we will be most interested.

A schematic representation of the polarization extremes - polarization resistance during active metal dissolution versus IR resistance across an insoluble corrosion product - is shown in Figure 3.

Under conditions of repetitive current reversal, any change in either degree or in rate of polarization signifies changes in the one of the three processes enumerated above. Of the three, only the third should provide any significant contribution. Thus, by evaluating such changes, we should be able to establish criteria for evaluating the environmental stability of a particular material in a given environment.

As "protective" films grow on bare or air-formed film covered metal substrates, there should be a regular increase in degree of polarization with each consecutive anodic cycle. Furthermore, the degree of polarization should progressively decrease as well, if the protective film is becoming more and more protective. Any change in this trend will be interpreted as an indication of development of instability in the system - a loss in ability of the system to resist the corrosive actions of the environment. We shall find, however, that with passive alloys like stainless steels, too high an electrical resistance leads to onset of pitting.

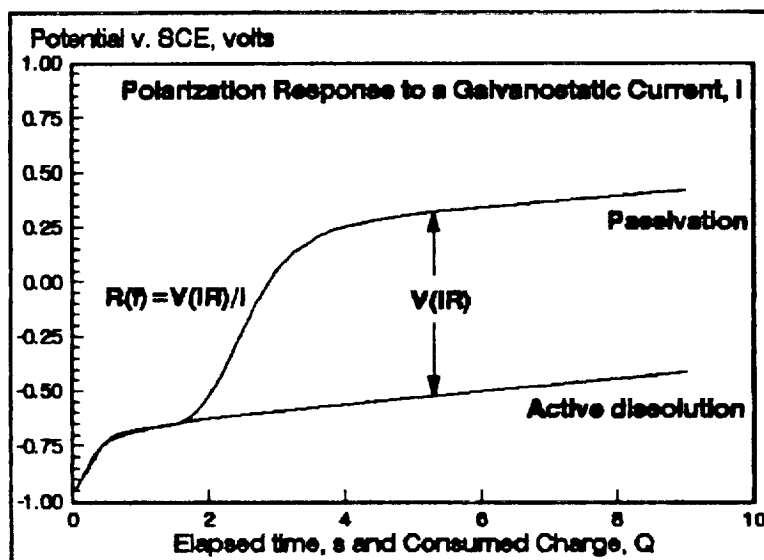


Figure 3 - Schematic representation of limiting cases in polarization behavior - metal dissolution v. insoluble corrosion product.

### 1.3 PROPOSED EXPERIMENTAL PROTOCOL

The CCRPV procedure requires that both magnitude of impressed current as well as its magnitude be specified - both these variables represent critical operating controls [Figure 4]. It would appear that current levels should correspond to maxima experienced during actual service exposure. However, this is not an easy selection to make. Cathodic currents seldom exceed the maximum for cathodic reduction of dissolved

oxygen - about  $10^{-3}$  amperes/cm<sup>2</sup> on steel surfaces. With concentration polarization, this value is reduced by several orders of magnitude - the 1 mA value represents an upper limit. Similarly, the duration of the current pulse represents the coulombic charge increment allowed to flow during the transient. Too short a time, and the system will not have time to respond or to polarize. Too long a period and the system will have changed too much - environmental compositions will have changed far in excess of realistic values. After considerable experimentation in c/5 natural seawater [natural seawater containing about 0.1 M Cl<sup>-</sup> ion] resulted in a  $\pm 6.25$   $\mu$ A current applied for 5 seconds. Finally, the total number of cycles to be included in the experiment had to be decided upon. Variation in this operating parameter is determined by what is necessary in order to get some idea of where the stability of the system is heading. Too few cycles and a clear direction is not obtained. Unfortunately, there was insufficient time for testing of optimum current/frequency/duration values.

In order to facilitate data acquisition and analysis, it was decided to develop a software program for use in running CCRPV experimentation on equipment in use in the NASA-KSC corrosion testing facilities. The procedure involved modification of commercial software prepared by Princeton Applied Research Corporation, the manufacture of the Model 273 potentiostat used in this research. Alteration of their CPCOM.T program was accomplished and is included in Appendix A at the end of this report.

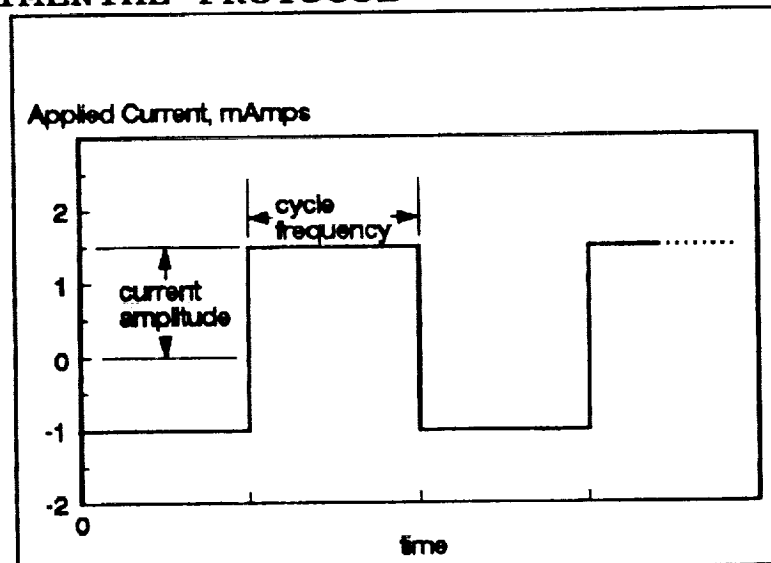


Figure 4 - Schematic of Experimental Procedure with respect to the RCRV control variables.

## 2.0 EXPERIMENTAL - MATERIALS and EQUIPMENT

### 2.1 Material

All experimentation was performed using specimens of 440C martensitic stainless steel provided by Pratt-Whitney Corporation of West Palm Beach, Florida. The nominal composition for this alloy is provided in Table I.

Table I - Elemental Composition for 440C Martensitic Stainless Steel Alloy Selected for this Study.

C	Mn	Si	Cr	P	S	Others
0.95-1.20	1.00	1.00	16.0-18.0	0.04	0.03	0.70 Mo

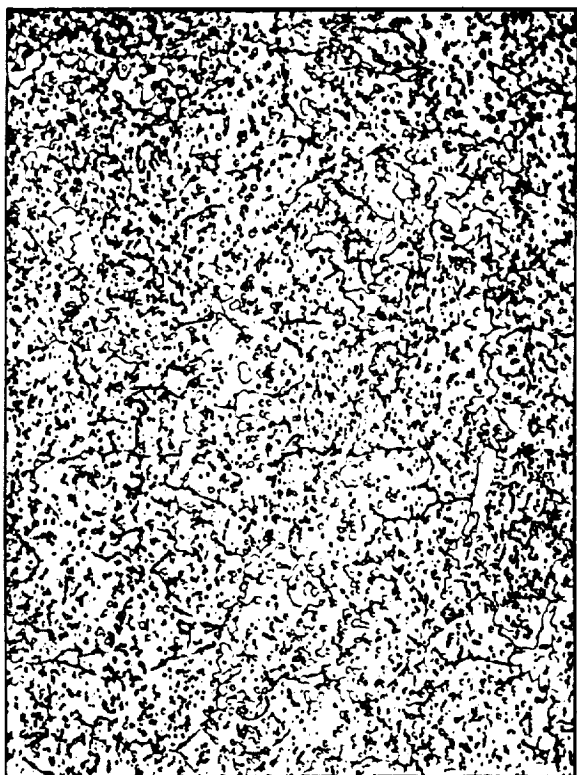


Photo 1 - Microstructure for PW#1, 400°F temper, super picral etch, 500x.

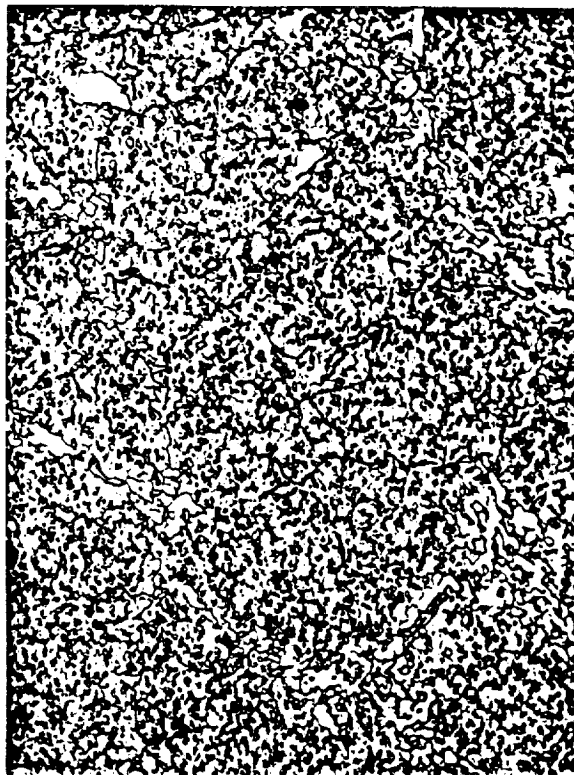


Photo 2 - Microstructure for PW#5, 750°F Temper, super picral etch, x500.



Photo 4 - Microstructure for PW#6, 1000F Temper, super picral etch, x500.

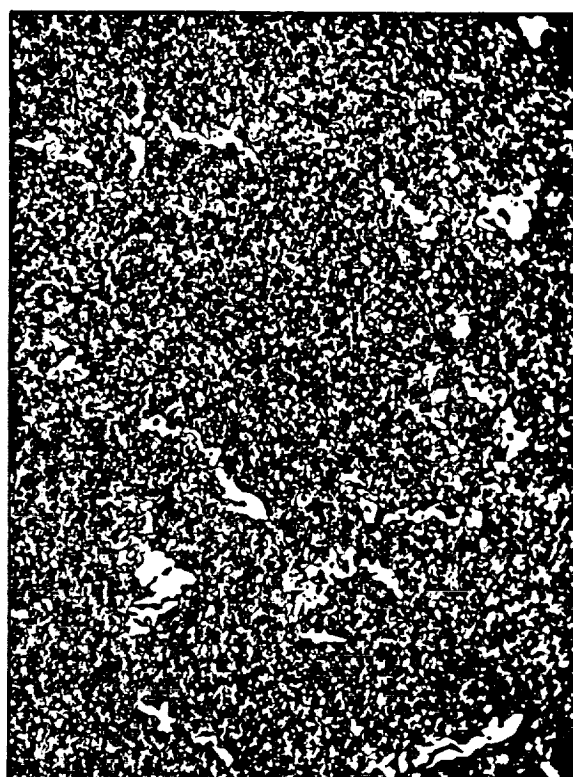


Photo 3 - Microstructure for PW# 7, 1250F temper, super picral etch, x500.

Duplicate specimens tempered at four different temperatures were received and their microstructures characterized. For each duplicate specimen set, one specimen was analyzed metallographically, while the other was used in the as-received condition for the electrochemical experimentation. When performing subsequent experiments, specimens were repolished according to the same procedure used for the metallographic specimens. Shown in Photos 1-4 are photomicrographs of specimen surfaces produced by mechanical rotary polishing through a series of silicon carbide metallographic polishing papers, 1 micron diamond paste on nylon cloth, finished with 0.3 and 0.05 micron alumina on felt. Etching was accomplished with a super picral etching medium.

Microstructures are consistent with conventional heat treatments described in the literature [Appendix B]. Of particular relevance to us will be the relative distributions of the primary carbide phase [large blocky light-colored phase] and secondary carbide phase [small circular light-colored phased] within the martensite matrix. Note that the primary carbide phase, produced during the initial quench from

the austenitizing temperature - therefore supposedly independent of tempering temperature, does appear to be somewhat different in the four tempers [Figures 5-8].

All experiments were performed in natural seawater, diluted with distilled water to a 1:5 concentration - approximately equal to a  $0.1 \text{ M Cl}^{-1}$  concentration. Solutions were stagnant, making no attempt to change the air saturated condition.

## 2.2 Equipment

The electrochemical cell used was a standard Greene cell furnished by EG&G Princeton Applied Research - counter electrodes [2] were graphite. 5/8-inch diameter, 3/16-inch thick specimens were designed to fit a standard PAR specimen holder in the PAR specimen holder. Electrochemical experimentation was performed using a PAR Potentiostat/galvanostat Model 273 in combination with an AT clone PC. Software was, as previously stated, an adaptation of PAR "Headstart, version 1.0, software.

## 2.3 Experimental Procedure

Following mounting in the cell specimen holder, specimens were placed in the electrochemical cell to which diluted seawater had already been added and allowed to stabilize for 10 minutes. Readings of open circuit [corrosion] potential were made immediately after placing in the cell, and at the 5 and 10 minute marks. After the stabilization interval, the CCRPV program was initiated. Following the 5 anodic/5 cathodic cycle sequence, the system was allowed to stabilize again for 10 minutes, with  $E_{\text{corr}}$  measurements made again at 5 minute intervals. Two more groupings of CCRPV perturbations were performed, following the same experimental protocol - a total of three groups of 5 current reversal sequences. Following the experimental procedure, the specimen was removed from the cell, and from the holder, cleaned, dried and retained for further experimentation.

Data was collected in a ASCII format, transferred to a standard LOTUS spreadsheet, collated and plotted. Named graphs were reprocessed using Lotus FREELANCE software, saved as TIFF files for incorporation into the WORDPERFECT, v. 5.1 text used in the writing of this report.

### 3.0 EXPERIMENTAL RESULTS and DISCUSSION

In Table II are listed the variations in corrosion or rest potentials which were recorded before and after each CCRPV group.

Table II - Corrosion Potential Data

Grp#	time	PW# 1	PW# 5	PW# 6	PW# 7
****	****	*****			
1	-10	-223	-227	-312	-260
	-5	-164	-244	-	-308
	0[b]	-161	-278	-406	-285 [?]
	0[a]	-153	-284	-421	-248
	-5	-175	-302	-451	-295
	-10	-181	-321	-476	-289
*****		*****			
2	0	-170	-331	-483	-209
	-5	-185	-342	-501	-289
	-10	-188	-353	-	-
*****		*****			
3	0	-177	-337	-507	-209
	-5	-190	-367	-517	-294
	-10	-192	-	-	-

Two features are evident: [1] There is a generalized progression in  $E_{corr}$  toward more negative values both before and after CCRPV runs; [2] There is a progressive shift in  $E_{corr}$  toward more negative values following CCRPV from group to group of CCRPV cycles. Such shifts could be due to either cathodic concentration polarization [diffusion limited  $O_2$  transport], to increases in anodic current density [passivity breakdown or pitting] or to both. It would appear that small changes in corrosion potential, on the order of 20-30 mV, are probably due to concentration polarization, while relatively larger changes [50-100 mV] are probably associated with passivity breakdown.

With respect to CCRPV experimentation, results will be treated in terms of the following comparisons between heat treatments:

- [1] Degree and rate of polarization for the 1st anodic cycle during the 1st group.
- [2] Degree and rate of polarization for the five anodic cycles within the 1st group for each temper.
- [3] Degree and rate of polarization for 1st anodic cycle of each group for each temper.
- [4] Same data treatment for the cathodic cycles [3 comparison classifications].

## Anodic Polarization Behavior

In Figure 5 are plotted the 1st anodic cycles of group for the 4 subject tempers in this study - 400, 750, 1000 and 1250°F - as a function of the square root of time. The fact that polarization kinetics would be linear with respect to  $t^{\frac{1}{2}}$  is significant in that the cause of the polarization - an electric resistance to the flow of current - is being limited by what appears to be diffusion control. Fick's 2nd Law for chemical diffusion would show the same order of reaction

kinetics. Notice that in Figure 5, only the polarization of the 400°F temper is linear with respect to  $t^{\frac{1}{2}}$ . This implies that the interfacial resistance developing in response to the flow of anodic current is being limited by diffusion of some species - if an anodic film is providing this resistance, its growth rate is being limited by the transport of some specie [or species] to or from the specimen/solution interface. Not only do the other three tempers not display diffusion limited kinetics, but their polarization rates are much higher. Except for specimen #6, the 1000°F temper, there would have been a direct correlation between polarization rate and degree of polarization and tempering temperature, with the higher temperatures producing higher DOP's and DOP rates. As it is, there appears to be a direct correlation between relative amount of primary carbide in the alloy microstructure [Photos 1-4] and polarization kinetics. It should be noted that the 1000° temper specimen, when removed from the cell, was found to be severely pitted. Occurrence of pitting during a CCRPV scan produces ambiguous results because the majority of the current flows out of the pits on the surface, a relatively small area. The remainder of the surface will show a disproportionate amount of polarization - thus the relative position of the 1000 temper as compared to the other three. The occurrence of pits on the surface of the 1000° temper is shown in Photo 5. Note that incidence of pitting is in proximity to primary carbide deposits within the alloy microstructure.

Comparing anodic behavior within the first CCRPV group, we see

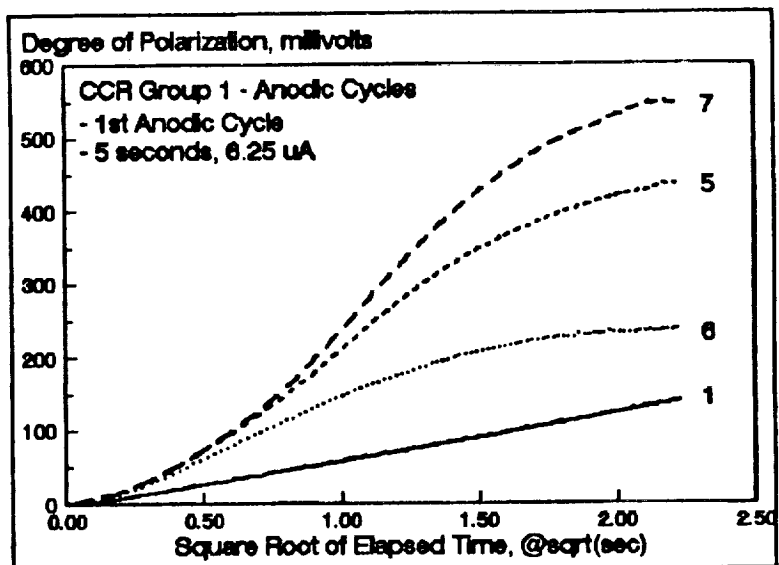


Figure 5 - Plot of Degree of Polarization  $[V(t)-V(o)]$  v.  $t^{\frac{1}{2}}$  for all 4 440C tempers - 1st anodic cycle, 1st CCRPV group.

that, although there is a slight [3-5 mV] increase in degree of polarization [DOP] from 1st to 5th cycle for the 400° temper,

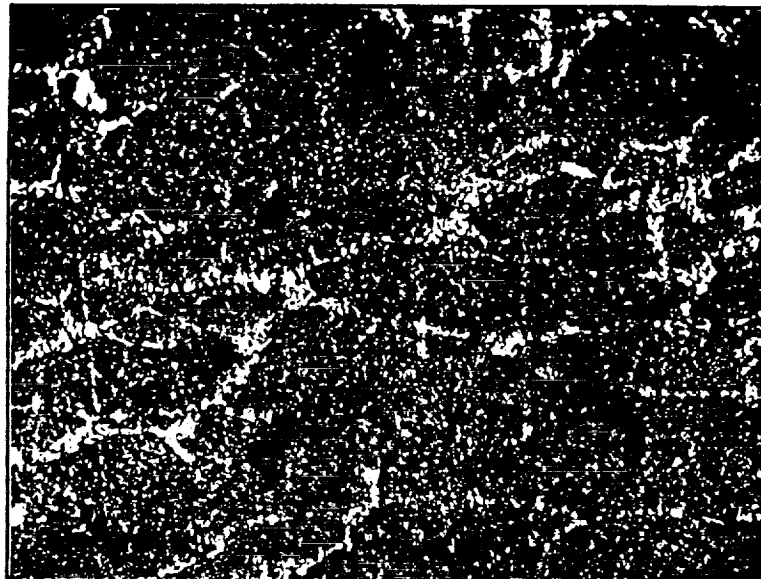


Photo 5 - Microstructure for PW#6, 1000° temper, after CCRPV run. Note dark areas which correspond to pits.

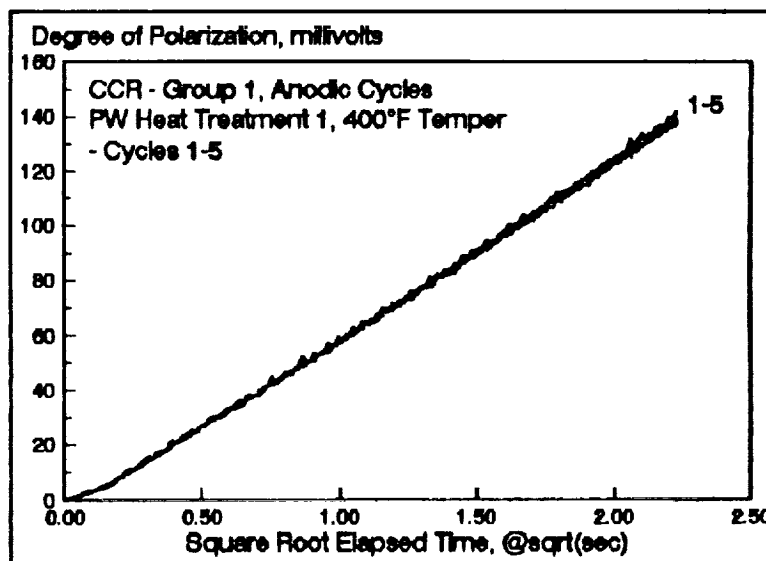


Figure 6 - 400° temper, group 1 anodic cycles.

there is no change in the delta DOP - the change in polarization from the beginning to the end of any given cycle - nor in the polarization rate [Figure 6]. The other three tempers do not

display the same constancy, with variations in both delta DOP and polarization rate - the 1000° temper, as you might have suspected, shows the most pronounced change [Figures 7-9].

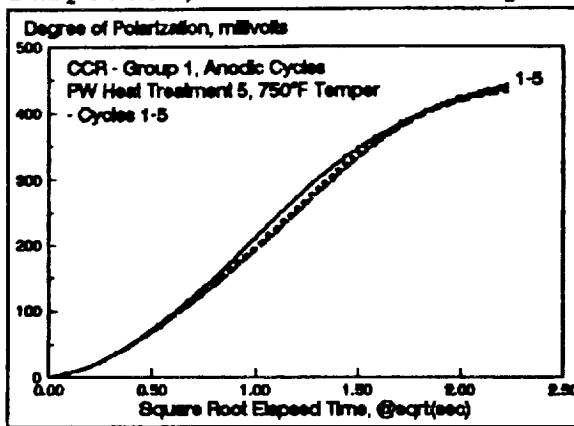


Figure 7 - 750° temper, group 1 anodic cycles.

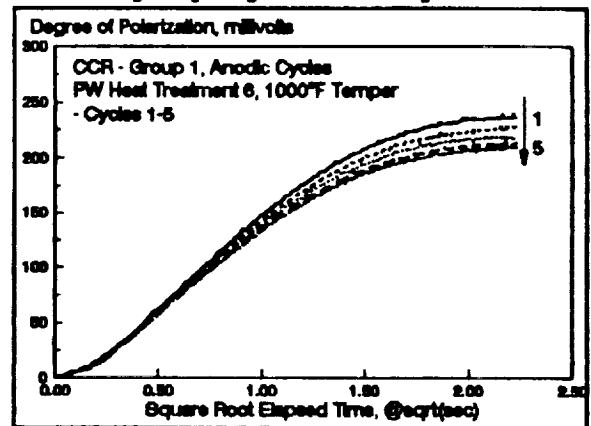


Figure 8 - 1000° temper, group 1 anodic cycles.

The consequences of cathodic polarization are shown in the Figure 10-14 series. It is important to note that although cathodic polarization does not, in itself, cause corrosion - just the opposite is true. Metals are not supposed to corrode under impressed cathodic current - that, after all, is the basis for "cathodic protection". However, cathodic polarization contributes to compositional changes in the solution adjacent to the metal surface - specifically, in the case of dissolved molecular oxygen reduction, to increases in

interfacial alkalinity or pH. At the very least, this pH change tends to offset acidity produced by the hydrolysis of metal cations produced by anodic dissolution of metal atoms. The synergistic interaction of both anodic and cathodic reaction products contributes to the production and maintenance of insoluble corrosion product layers at metal/solution interfaces - to passive behavior. Thus, in a very real sense, the results of the first cathodic polarization cycle will affect what happens during the immediately preceding anodic cycle, and so on.

Cathodic polarization behavior follows the same pattern established for anodic behavior - increases in tempering temperature result in an increase in both cathodic DOP and in cathodic polarization rates [Figure 10]. Note again, that in the

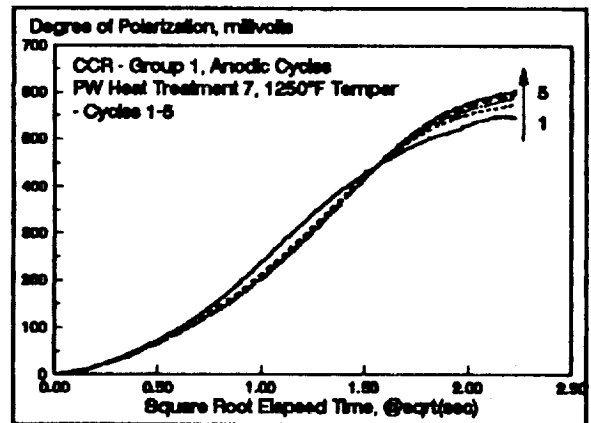


Figure 9 - 1250° temper, group 1 anodic cycles.

case of the 400° temper, that polarization appears to follow diffusion limited mass transport kinetics while the others do not. For whatever it is worth, both anodic and cathodic polarization can be linearized by plots  $\Delta DOP$  as a function of  $t^{1/2}$  where  $x$  can have values between 0.600 and 0.750. The mechanistic significance in terms of what process or processes control has yet to be established.

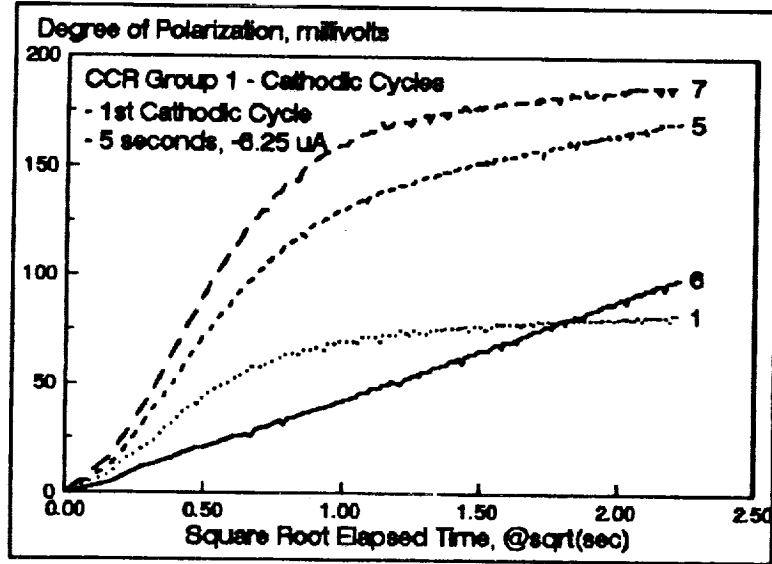


Figure 10 - Group 1, 1st cathodic cycles for 400°, 750°, 1000° and 1250° temps.

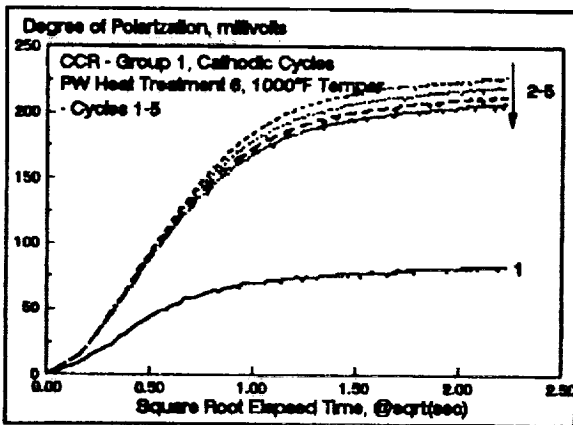


Figure 11 - 1000° temper, group 1 cathodic cycles.

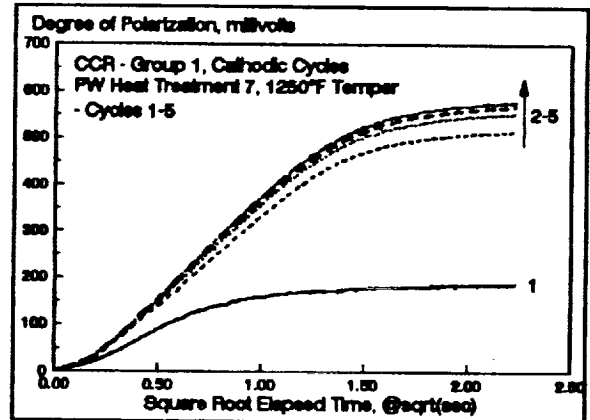


Figure 12 - 1250° temper, group 1 cathodic cycles.

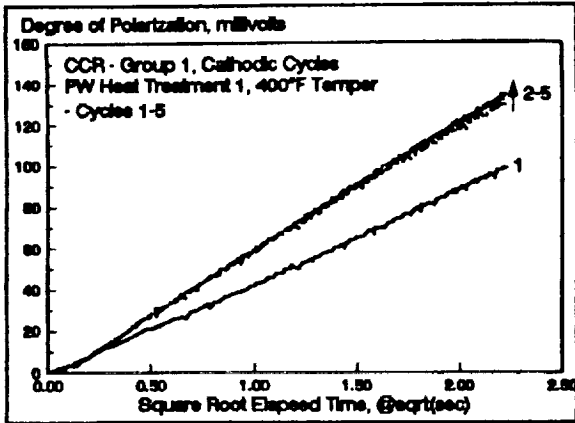


Figure 13 - 400° temper, group 1 cathodic cycles.

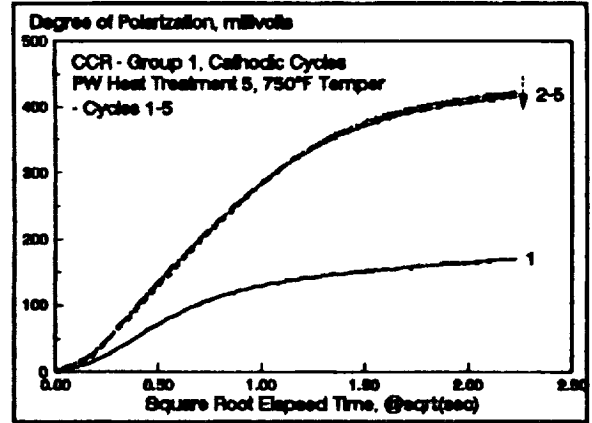


Figure 14 - 750° temper, group 1 cathodic cycles.

When comparing the 5 cathodic cycles for group 1, it is immediately obvious that the 1st cycle is different than all others - both in a lower DOP and polarization rate. Why this behavior during the 1st cycle is not clear - perhaps the change from bulk interfacial pH [about 8.5] is most pronounced during the 1st cycle. It is also possible that any corrosion product produced during the subsequent anodic cycle is never completely removed during later cathodic cycles. Whatever, the difference is there. It is also interesting to note, that except for our 1000° temper anomalous behavior, there appears to be a regular increase in cathodic polarizability with increasing tempering temperature. Whatever is changing about the microstructure is clearly making the cathodic reduction process more difficult, requiring increasing voltages to be induced in response to our -6.25  $\mu$ A impressed current level [Figures 10-14].

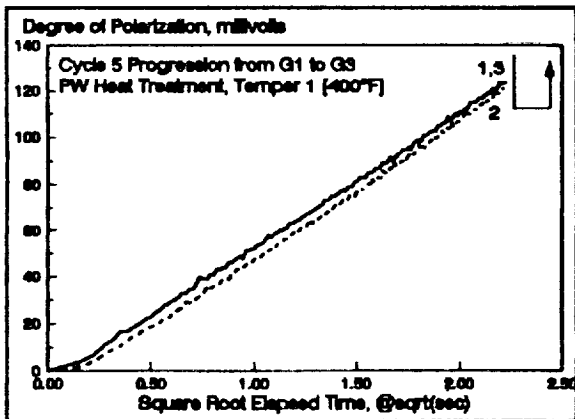


Figure 15 - Comparison of 5th anodic cycles in groups 1-3 for temper 400°.

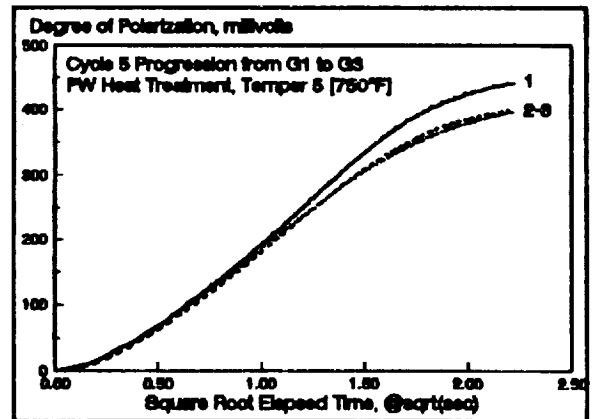


Figure 16 - Comparison of 5th anodic cycles for groups 1-3 for temper 750°.

When comparing 5th anodic cycles for groups 1-3 [Figures 15-18], we notice that the 400° and 750° tempers show virtually no change in polarization behavior [Figures 15 and 16].

For the 1000 and 1250°F tempers, however, there are variations. The 1000°F temper material, which fails to repassivate during cathodic cycles, shows a large drop in anodic polarizability from the 5th cycle in group 1 to the 5th cycle in

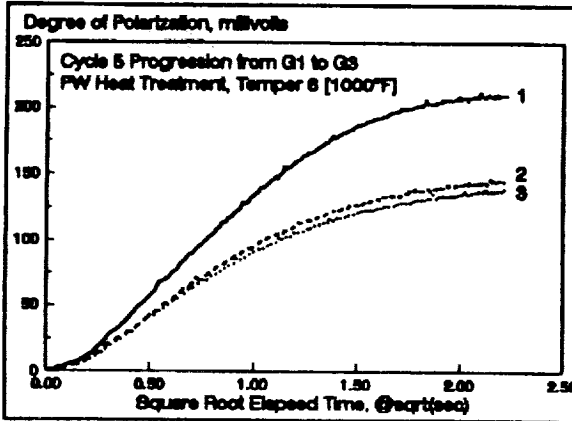


Figure 18 - 1000° temper, comparison of 5th anodic cycles for groups 1-3.

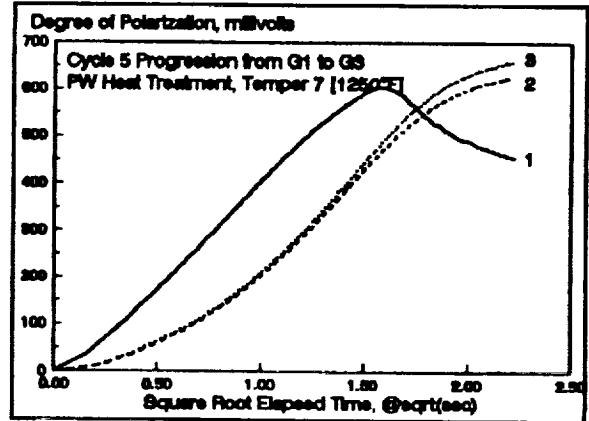


Figure 17 - Temper 1250, comparison of 5th anodic cycles, groups 1-3.

group 2, with little change through group 3. It is interesting to compare this behavior with that of the 1250 temper, which suffers breakdown at the tend of the 5th cycle [maxima in anodic polarization] but repassivates and shows no loss in corrosion resistance through groups 2 and 3.

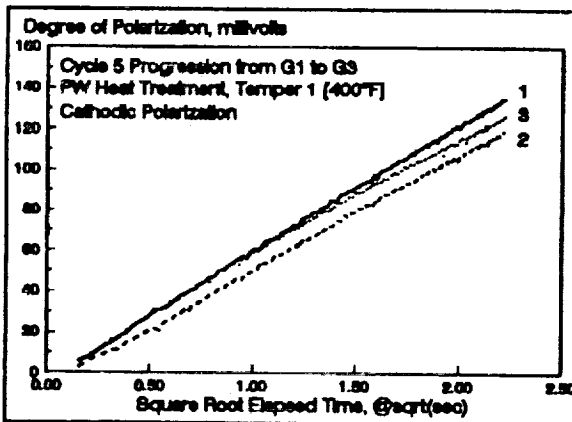


Figure 19 - 400 temper, comparison of 5th cathodic cycles, groups 1-3.

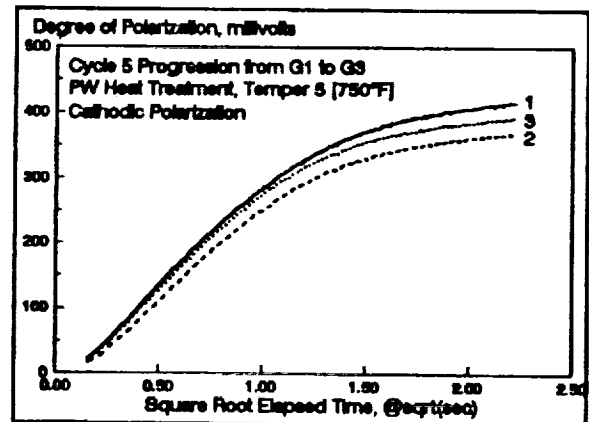


Figure 20 - 750 temper, comparison of 5th cathodic cycles for groups 1-3.

Looking at progressive changes in cathodic polarization behavior, the results again seem to parallel anodic behavior. As Figures 19 and 20 show, little variation in 5th cycle cathodic behavior occurs from group 1 to 3 for either the 400 or 750 temper alloys. Likewise, there is little effect on the reaction order either. Cathodic polarization rates obey  $t^{1/2}$  kinetics throughout the exposure period.

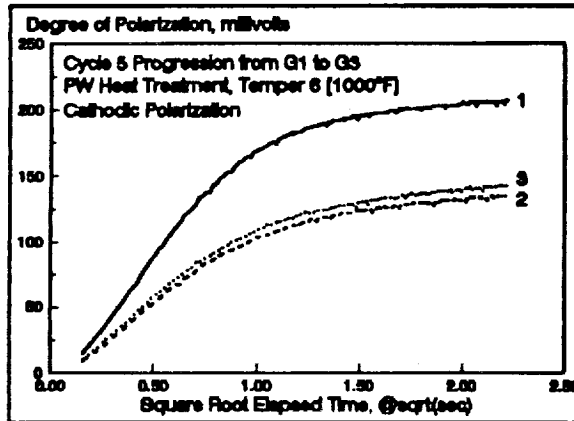


Figure 21 - 1000° temper - comparison of 5th cathodic cycles for groups 1-3.

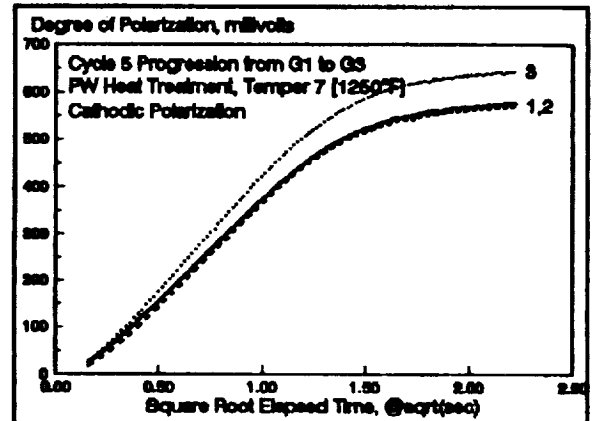


Figure 22 - 1250° temper - comparison of 5th cathodic cycles for groups 1-3.

Finally, variations in cathodic polarization behavior for the 1000 and 1250° tempers also parallel their anodic counterparts.

#### 4.0 CONCLUSIONS

The CYCLIC CURRENT REVERSAL POLARIZATION VOLTAMMETRY technique offers a simple, inexpensive method for distinguishing, even quantifying the relationship between alloy microstructure and localized corrosion resistance. The study presented here utilizes the tempering temperature as a variable - increases in this temperature for tempering of martensite is supposed to alter the carbide/ferrite fraction of the microstructure and increase alloy toughness. What happens to the corrosion resistance was then the subject of this research.

Increasing the tempering temperature results in a greater resistance to both anodic and cathodic polarization - the consequences appearing to adversely affect corrosion resistance. Although an increase in temperature where the unstable martensite to stable dispersions of carbide in ferrite transformation occurs should result in changes within the secondary carbide/ferrite microconstituent, this is not apparent. Rather, there appears to be little change in the carbide/ferrite microconstituent and an increase in the relative amount of the primary carbide phase at the prior austenite grain boundaries. Just why this increase should result in boundary layers which afford greater resistance to passage of electric current is not clear, but there is no question that the 1000°F temper displays an extremely poor resistance to onset of pitting than does its 400° counterpart.

## 5.0 RECOMMENDATIONS FOR FUTURE WORK

Although the technique appears to be sensitive to variations in microstructure, it will be necessary to quantify relationships a bit more. For instance, what are the specific causes for changes in the various CCRPV output parameters? What would changes in temperature, dissolved oxygen concentration, solution pH, salinity, etc. produce?

Secondly, Pratt and Whitney are interested in determining the effect of other microstructural modifications - namely, quenching in oil with development of a high carbon "white layer" on the material surface. Oil quenches will result in less severe residual stresses being incorporated into the alloy. In order to eliminate any negative consequences of the "white layer", the effect of nickel plated surfaces prior to austenization are to be evaluated. These tests, a continuation of the work begun this summer, will be finished at the University of Florida during the coming academic year.

## 6.0 APPENDICES

### 6.1 Appendix A - CCRPV menu [CCRPVCOM]

```
*****
DCL ' M273 DEFAULT PARAMETERS
I/E -4 ' 100 uA FULL SCALE CURRENT OUTPUT
MODE 1 ' GALVANOSTATIC MODE
BIAS 0 ' NO OFFSET, CURRENT=0 AT START
MR 2 ' 8000 COUNTS=2V ON MOD DAC
MM 2 ' ARBITRARY WAVEFORM MODE
SCV 2 ' SOURCE CURVE #2
DCV 0 ' DESTINATION CURVE #0
FP 0;LP 2000 ' 2000 POINTS FROM 1ST TO LAST POINT
TMB 25000 ' 50 SECOND RUN
S/P 1 ' ONE READING PER POINT
PAM 0 ' NO AVERAGING
INITIAL 0 0 ' ZERO CURRENT 1ST POINT
VERTEX 1 -500 ' A STEP OF 1/8 X FULL SCALE CURRENT RANGE
VERTEX 199 -500 '
VERTEX 200 500 ' CURRENT REVERSAL [- TO +]
VERTEX 399 500 '
VERTEX 400 -500 '
VERTEX 599 -500 '
VERTEX 600 500 '
VERTEX 799 500 '
VERTEX 800 -500 '
VERTEX 999 -500 '
VERTEX 1000 500 '
VERTEX 1199 500 '
VERTEX 1200 -500 '
VERTEX 1399 -500 '
VERTEX 1400 500 '
VERTEX 1599 500 '
VERTEX 1600 -500 '
VERTEX 1799 -500 '
VERTEX 1800 500 '
VERTEX 1999 500 '
VERTEX 2000 -500 '
ASM ' ASSEMBLE ARB WAVE FORM INTO SCV
SIE 2 ' POTENTIOMETRY-MEASURE POTENTIAL
INTRP 0 ' CLEAN STEP
EGAIN 5 ' 2.000 VOLT FULL SCALE POTENTIAL MEASUREMENT
NC ' PRELOAD MOD DAC WITH 1ST POINT IN ARB WAVEFORM
CELL 1 ' TURN CELL ON
P 5 ' PAUSE 5 SECONDS AT CURRENT = 0
TC ' TAKE CURVE
WCD;CELL 0 ' CELL OFF AFTER CURVE DONE
GOSUB 51000: STOCK SUBROUTINE - TRANSFERS DATA
GOSUB 52000: STOCK SUBROUTINE - STORES DATA
*****
```

## 6.0 APPENDICES

6.2 Appendix B - Microstructures and Heat Treatments for 440C  
"Heat Treater's Guide - Standard Practices  
and Procedures for Steel, Paul M.  
Unterweiser, ASM, Metals Park, 1982  
[pp 438-9]

## 440C

**Chemical Composition. AISI and UNS:** Nominal. 0.95 to 1.20 C, 1.00 Mn max, 0.040 P max, 0.030 S max, 1.00 Si max, 16.00 to 18.00 Cr, 0.75 Mo max

**Similar Steels (U.S. and/or Foreign).** UNS S44004; AMS 5618, 5630; ASTM A276, A314, A473, A493, A580; FED QQ-S-763; MIL SPEC MIL-S-862; SAE J405 (51440 C); (W. Ger.) DIN 1.4125; (Jap.) JIS SUS 440C

**Characteristics.** Highest hardness of hardenable stainless steels. Good corrosion resistance, particularly in hardened and tempered condition. Quenched in oil or air. Can be martempered. Can be full, process, or isothermal annealed. Magnetic in all conditions. Low machinability. Used for bearings, nozzles, valve parts, and wear parts of pumps

**Forging.** Start forging at 1900 to 2150 °F (1040 to 1175 °C). Do not forge below 1750 °F (955 °C). Cool slowly from finishing temperature. Anneal

### Recommended Heat Treating Practice

**Normalizing.** Do not normalize

**Annealing.** Can be process, isothermal, or full annealed:

- **Process anneal** in subcritical temperature range of 1250 to 1400 °F (675 to 760 °C) for hardness of 98 HRB to 23 HRC. Use clean, rectified salt bath or an atmosphere that is compatible with this temperature range. Soaking and softening time depend on section size of the work. Air cool
- **Isothermal anneal** by heating to 1550 to 1650 °F (845 to 900 °C). Cool slowly to 1275 °F (690 °C). Hold for 4 hr. Hardness, approximately 25 HRC
- **Full anneal** at 1550 to 1650 °F (845 to 900 °C). Cool at a rate not faster than 30 to 40 °F (17 to 22 °C) per hour to 1100 °F (595 °C), after which cooling rate does not affect hardness. Avoid decarburization. Can use atmospheric protection in the form of a vacuum, the inert gases argon or helium (both expensive), or nitrogen. All should have dew point below -60 °F (-51 °C). For endothermic-generated atmosphere, hold dew point in the 0.95 to 1.20 carbon range for the annealing temperature used. Annealed hardness, 98 HRB to 25 HRC. Full annealing, expensive and time consuming, should not be used except as required for subsequent forming or difficult specialized metal cutting operation

**Hardening.** Atmospheric protection rules for annealing apply to hardening. Parts must be completely clean and free

of oil and shop contamination. Thermal conductivity is significantly lower than that of carbon and alloy steels. High stresses during rapid heating may cause warpage and cracking in delicate or intricate parts. Preheat at 1400 to 1450 °F (760 to 790 °C), only long enough to equalize temperature in all sections. Extremely delicate or intricate parts would benefit from an additional prior preheat at 1000 °F (540 °C). Austenitize at 1850 to 1950 °F (1010 to 1065 °C). Use upper end of range for larger sections or where maximum corrosion resistance and strength are required. Soaking time of 30 to 60 min is adequate for sections up to ½ in. (13 mm). Allow an additional 30 min for each additional inch or fraction thereof. Double soaking time if parts have been full or isothermal annealed. If process annealed above 1300 °F (705 °C), increase soaking time by about 50%. Quench in oil or air. Oil preferred, because it guarantees maximum corrosion resistance and ductility. Martempering in hot oil or salt is suitable because of high hardenability. As-quenched hardness, approximately 60 to 62 HRC minimum

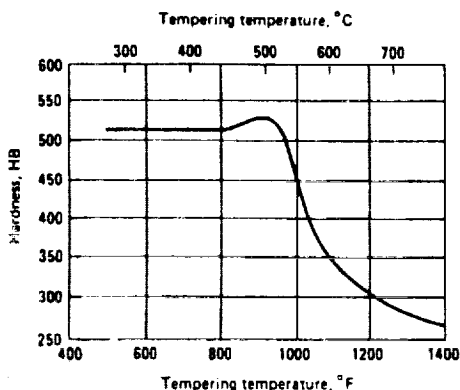
**Stabilizing.** For minimum retained austenite and maximum dimensional stability, use subzero treatment at -100 ± 20 °F (-74 °C). This should incorporate continuous cooling from the austenitizing temperature

**Tempering.** Temper at 325 °F (165 °C) or higher, for minimum hardness of 60 HRC. Temper at 375 °F (190 °C), for 58 HRC minimum; at 450 °F (230 °C), for 57 HRC minimum; and at 675 °F (355 °C), for hardness approximately 52 to 56 HRC. Double tempering beneficial. Cool to room temperature between tempers

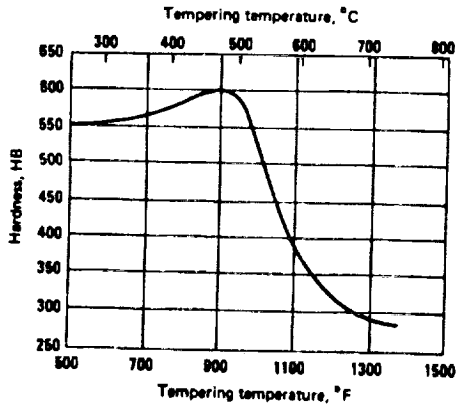
**Nitriding.** Can be nitrided to case depth of 0.008 in. (0.203 mm) in 48 hr. For further information, see type 410

### Recommended Processing Sequence

- Forge
- Anneal
- Rough machine
- Stress relieve
- Finish machine
- Preheat
- Austenitize
- Quench
- Stabilize (not mandatory, but beneficial)
- Temper
- Final grind to size
- Nitride (if required)

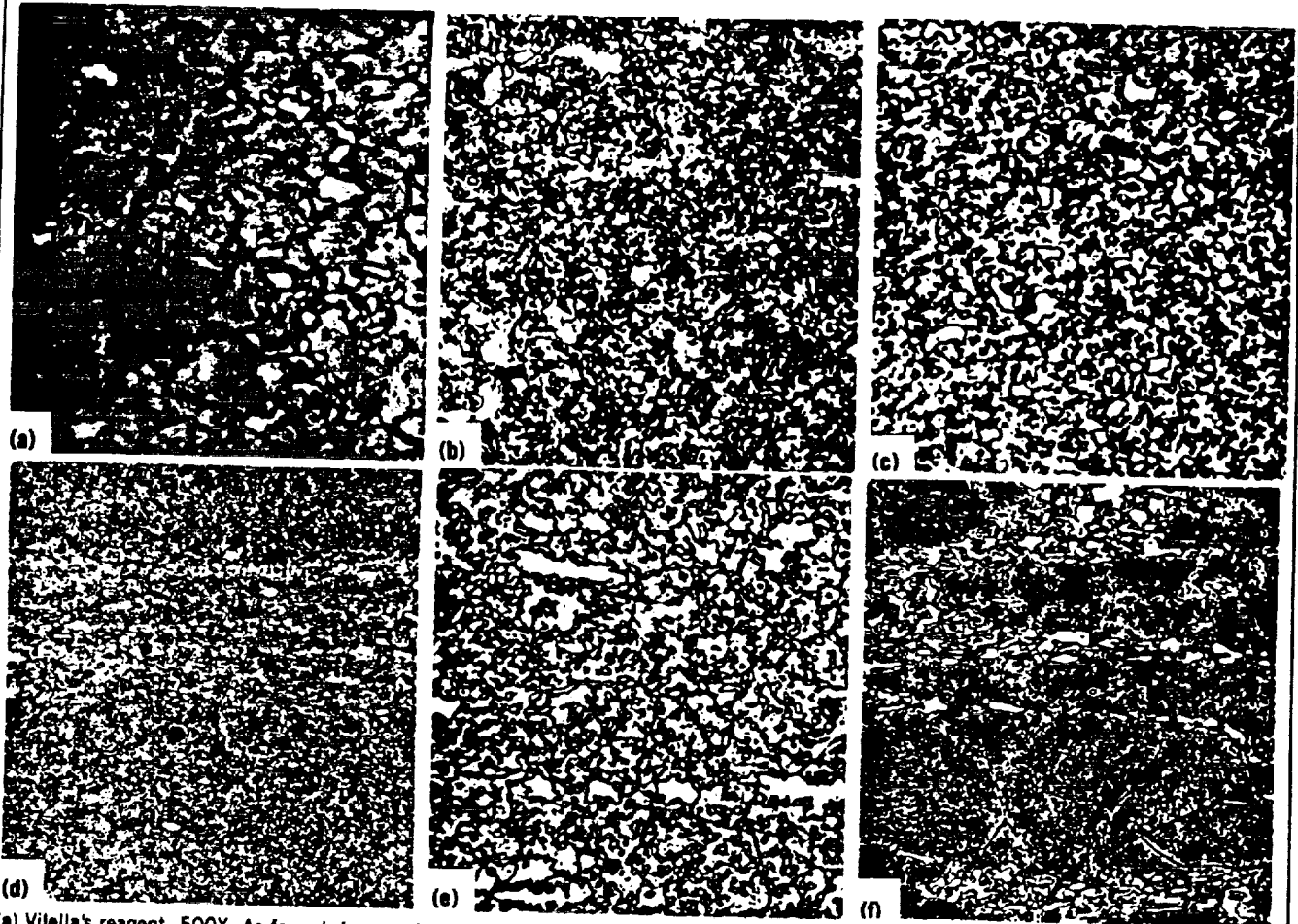


**440C: Hardness Versus Tempering Temperature.** Composition: 1.020 to 1.044 C, 0.40 to 0.48 Mn, 0.017 to 0.019 P, 0.010 to 0.011 S, 0.18 to 0.31 Si, 16.90 to 17.18 Cr, 0.24 to 0.54 Ni, 0.50 to 0.64 Mo. Heat treated at 1700 °F (925 °C), 1 hr. Oil quenched at 150 to 200 °F (66 to 94 °C). Double stress relieved at 350 °F (175 °C), 15 min. Water quenched. Tempered 2 hr. Heat treated, 0.550-in. (14-mm) round. Tested, 0.505-in. (12.8-mm) round. (Source: Republic Steel)



**440C: Hardness Versus Tempering Temperature.** Composition: 1.02 C, 0.48 Mn, 0.017 P, 0.011 S, 0.18 Si, 16.90 Cr, 0.54 Ni, 0.64 Mo. Heat treated at 1900 °F (1040 °C), 2 hr. Oil quenched at 150 to 200 °F (66 to 94 °C). Double stress relieved at 350 °F (175 °C), 15 min. Water quenched. Tempered 2 hr. Heat treated, 0.385-in. (9.78-mm) round. Tested, 0.375-in. (9.53-mm) round. At 500 to 1000 °F (260 to 540 °C). Also, heat treated, 0.550-in. (14-mm) round. Tested, 0.505-in. (12.8-mm) round. At 1100 to 1400 °F (295 to 760 °C). (Source: Republic Steel)

#### 440C: Microstructures



(a) Vilella's reagent, 500X. As forged. Large primary carbide particles. Heavy carbide precipitation at grain boundaries. Secondary carbide particles. Matrix predominantly retained austenite. (b) Vilella's reagent, 500X. Forging annealed at 1600 °F (870 °C). Furnace cooled to 200 °F (94 °C) in 48 hr. Air cooled. Large particles of primary and spheroidized particles of secondary carbide. Ferrite matrix. (c) Vilella's reagent, 500X. Forging hardened by austenitizing at 1850 °F (1010 °C), 1 hr. Air cooled. Tempered at 450 °F (230 °C), 2 hr. Large primary and tempered secondary carbide particles. Martensite matrix. (d) Vilella's reagent, 100X. Forging, hardened and tempered. Band of carbide particles and matrix. (e) Super picral, 500X. Bar, preheated at 1400 °F (760 °C), ½ hr. Austenitized at 1875 °F (1025 °C), ½ hr. Air cooled martensite matrix. (f) Vilella's reagent, 200X. Bar, austenitized at 1850 to 1925 °F (1010 to 1050 °C). Oil quenched. Tempered at 375 °F (190 °C). Segregated stringers of primary carbide (light) and dispersed secondary carbide particles. Tempered martensite matrix. (Source: *Metals Handbook*, 8th ed., Vol 7, American Society for Metals, 1972)

